

Design and evaluation of a novel series of 2,3-oxidosqualene cyclase inhibitors with low systemic exposure, relationship between pharmacokinetic properties and ocular toxicity

Marie-Hélène Fouchet,^{a,*} Frédéric Donche,^a Christelle Martin,^a Anne Bouillot,^a Christophe Junot,^{b,†} Anne-Bénédicte Boullay,^c Florent Potvain,^c Sylvie Demaria Magny,^c Hervé Coste,^c Max Walker,^d Marc Issandou^c and Nérina Dodic^a

^aDepartment of Medicinal chemistry, Laboratoire GlaxoSmithKline, 25-27 Avenue du Québec, 91951 Les Ulis, France

^bDepartment of Drug Metabolism and Pharmacokinetics, Laboratoire GlaxoSmithKline, 25-27 Avenue du Québec, 91951 Les Ulis, France

^cDepartment of Biology, Laboratoire GlaxoSmithKline, 25-27 Avenue du Québec, 91951 Les Ulis, France

^dCVU Strategy and Operations, Laboratoire GlaxoSmithKline, 709 Swedeland Road, King of Prussia, PA, USA

Received 21 November 2007; revised 9 April 2008; accepted 16 April 2008

Available online 18 April 2008

Abstract—We describe the discovery of novel potent inhibitors of 2,3-oxidosqualene:lanosterol cyclase inhibitors (OSCi) from a focused pharmacophore-based screen. Optimization of the most tractable hits gave a series of compounds showing inhibition of cholesterol biosynthesis at 2 mg/kg in the rat with distinct pharmacokinetic profiles. Two compounds were selected for toxicological study in the rat for 21 days in order to test the hypothesis that low systemic exposure could be used as a strategy to avoid the ocular side effects previously described with OSCi. We demonstrate that for this series of inhibitors, a reduction of systemic exposure is not sufficient to circumvent cataract liabilities.

© 2008 Elsevier Ltd. All rights reserved.

1. Introduction

Hypercholesterolemia constitutes a major-risk factor for coronary artery disease which is the leading cause of death and a major source of morbidity in developed countries.¹ The benefits of lowering cholesterol level via inhibition of cholesterol biosynthesis have been clearly demonstrated in humans by the Statin class of drug.^{2,3} Statins are inhibitors of HMGCoA reductase and inhibit at an early rate-limiting step the cholesterol biosynthetic cascade. This results in decreased levels of cholesterol and depletion of mevalonate, which may be the cause of Statin side effects such as myopathy at high doses.⁴ In our search for lipid-lowering drugs, we targeted an alternative point of inhibition of cholesterol production. 2,3-oxidosqualene:lanosterol cyclase (OSC)

is a key enzyme in the cholesterol biosynthesis pathway and controls the conversion of 2,3-mono-epoxysqualene to lanosterol. OSC is located downstream from HMG-CoA and its inhibition should be free of isoprenoid depletion issues.

Several OSC inhibitors (OSCi) have been reported in the literature, showing in vitro and in vivo potency,^{5–9} demonstrating that OSC inhibition can deliver drugs with profound lipid-lowering effects. Moreover, treatment with OSCi was not associated with the development of a range of side effects that are reported commonly for HMGCoA reductase inhibitors, such as gall bladder, testicular and neurological changes.¹⁰ However, other types of toxicological issues have been reported including skin and epididymal changes in the dog, as well as severe cataract formation in dogs and rodents.¹⁰

U18666A, probably the first reported OSCi,¹¹ is known to induce cataracts.¹² U18666A was shown to intercalate into a lens lipid model membrane, and it has been hypothesized that the cataractogenic effect of OSCi could be related to direct perturbation of lens membrane

Keywords: 2,3-Oxidosqualene:lanosterol cyclase; Hypercholesterolemia; Pharmacophore; OSC inhibitor.

* Corresponding author. Tel.: +33 1 69 29 61 07; e-mail: marie-helene.fouchet@gsk.com

† Present address: Laboratoire d'Etude du Métabolisme des Médicaments, CEA—Saclay, France.

structure and function.¹³ If this were the case, then structural modification might be a way to decrease the impact of OSCi on cataract induction. Two members of the aminopyrimidine series of OSCi, with very different structure to U18666A, have also been shown to induce equatorial cataracts in the mouse and dog.¹⁰ It has been suggested that for this series of inhibitors, the mechanism of cataract formation may be rather due to inhibition of cholesterol in the lens than to lens-membrane perturbation. The critical role of lens sterol metabolism in the maintenance of lenticular transparency has already been demonstrated.^{14,15} Large amounts of synthesized cholesterol are required for the elongation of cell fibers and therefore, the inhibition of the cholesterol pathway leads to decreased membrane production and disturbed fiber cell growth. Recently, the histopathologic findings in hamster and dog associated with the administration of three different OSCi were published.¹⁶ The treatment (less than four weeks) produced a similar spectrum of eye lesions to those previously described for other compounds of this pharmacological class. However, in this study, dermal and ocular side effects were less pronounced when the dogs were given a cholesterol-rich diet, suggesting that observed changes were related to the inhibitory effect on cholesterol biosynthesis and not to intrinsic toxicity. The authors considered that the adverse effects described were due to supra-pharmacological effects on OSC at high dose levels, and that a decrease in systemic exposure could reduce these adverse effects. Such a trend was previously observed with various HMGCoA reductase inhibitors in the dog for which a strong relationship was demonstrated between plasma drug level and the cataractogenic potential.^{17,18} Unfortunately, no data concerning the exposure levels compared with those seen at pharmacological doses were published with the two previously described toxicological studies of OSCi.^{10,16}

Based on the above hypothesis, our goal was to evaluate the possibility of developing an OSC inhibitor free of cataract liability as a result of reduced peripheral exposure. A program was initiated to identify a set of small molecules inhibiting OSC both in vitro and in vivo in order to select compounds with different peripheral exposure parameters and to take them forward into toxicological studies.

2. Results and discussion

2.1. Pharmacophore-based focused screen

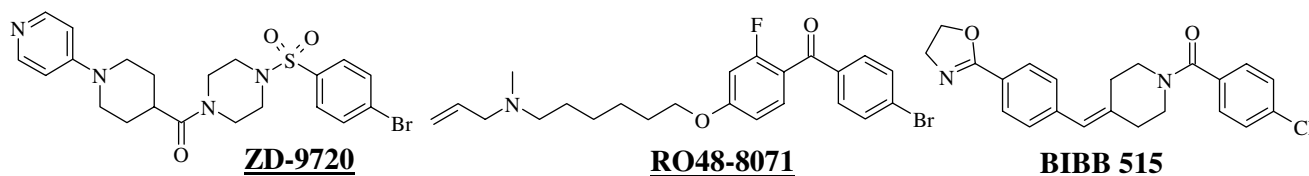
At the outset of this work no crystal structure of human oxidosqualene cyclase had been published, but the large

amount of SAR data available in the literature at that time encouraged us to favor a pharmacophore-based screening approach rather than high throughput screening. The pharmacophore was generated from three well-characterized and structurally diverse published OSCi (Scheme 1) presenting the chemical features assumed to be necessary for potency⁹: a physiologically protonated amine at one extremity of the molecule, a small lipophilic electron-withdrawing substituent on an aryl ring at the opposite extremity, and an electrophilic group incorporated close to this terminal aryl. The distance between the amine and the aryl is certainly important and was held somewhat constant, but the nature of the spacer was permitted to vary. Finally we assumed an extended conformation of the inhibitor as suggested by the chair-boat-chair conformation of both intermediate and reaction product of the OSC enzymatic reaction and by the binding mode of RO48-8071 in squalene:hopene cyclase, first hypothesized by modeling^{19a} and further confirmed by X-ray co-crystallization studies.^{19b} A five-point pharmacophore that fulfilled these criteria was selected. As shown in Figure 1, a hydrogen-bond acceptor feature was preferred to a protonated amine, and generic hydrophobic features replaced the aromatic ring and the electron-withdrawing group in order to enable a more diverse selection of compounds. A search in the GSK corporate compound collection identified 4300 virtual hits. Standard 'lead-like' filters were applied to give a preferred set of 3000 compounds for screening. One hundred and ten compounds showed some inhibition of OSC, and the 21 most potent, with an IC₅₀ less than 1.5 μ M, were considered for further profiling. We focused a medicinal chemistry program on the most tractable and novel series represented by compound 1, displayed in Scheme 2.

Recently the crystal structure of human OSC co-crystallized with RO48-8071 was published.²⁰ The main features defining our pharmacophore are coherent with the binding mode of RO48-8071 as observed in the crystal structure: the basic nitrogen and the carbonyl are hydrogen-bonded with the protein and the terminal phenyl group situated in an electron-rich pocket makes an electron-deficient aromatic ring an optimal group. The overall shape of the inhibitor is extended but not to the extent used in our model. As a consequence the distance between the hydrogen-bond donor and acceptor features may have been slightly over-estimated in our 3D searches.

2.2. Chemistry

4-Bromophenethylamine **2** was first coupled with the appropriate benzene sulfonyl chloride and then submit-



Scheme 1. Known OSCi used as starting points for the pharmacophore model generation.

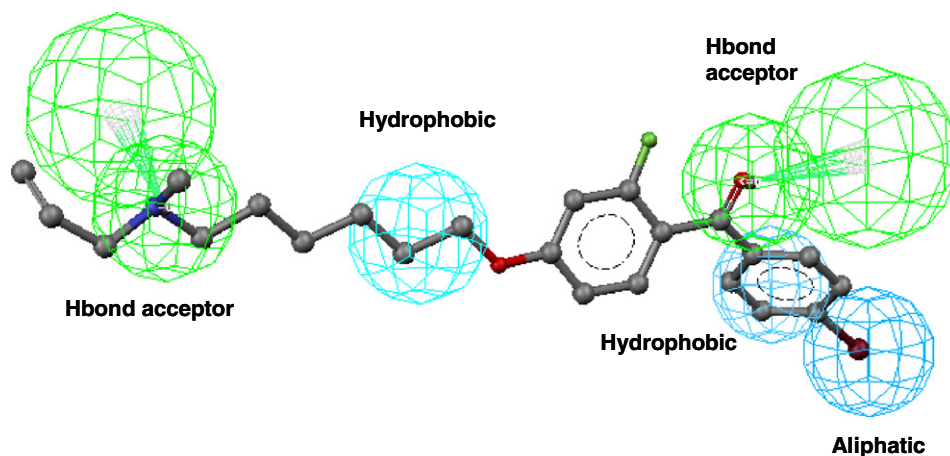
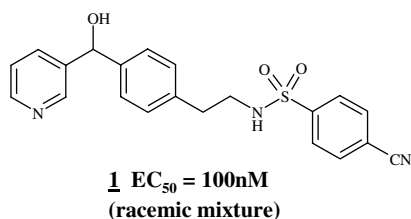


Figure 1. Mapping of RO48-8071 on the selected five points pharmacophore model of OSCi.



Scheme 2. Compound 1.

ted to Suzuki coupling. Reductive amination of the resulting biphenyl carboxaldehyde **4** with *N,N*-dimethylamine or pyrrolidine afforded compounds **10–12** (Scheme 3).

Starting from the substituted benzaldehydes **5**,^{21–23} reductive amination with *N*-Boc-piperazine followed by the acidic cleavage of the *t*-Boc group led to the intermediate **6**, which was submitted to coupling reaction with the appropriate benzene sulfonyl chloride or benzene carbonyl chloride to afford the desired compounds.

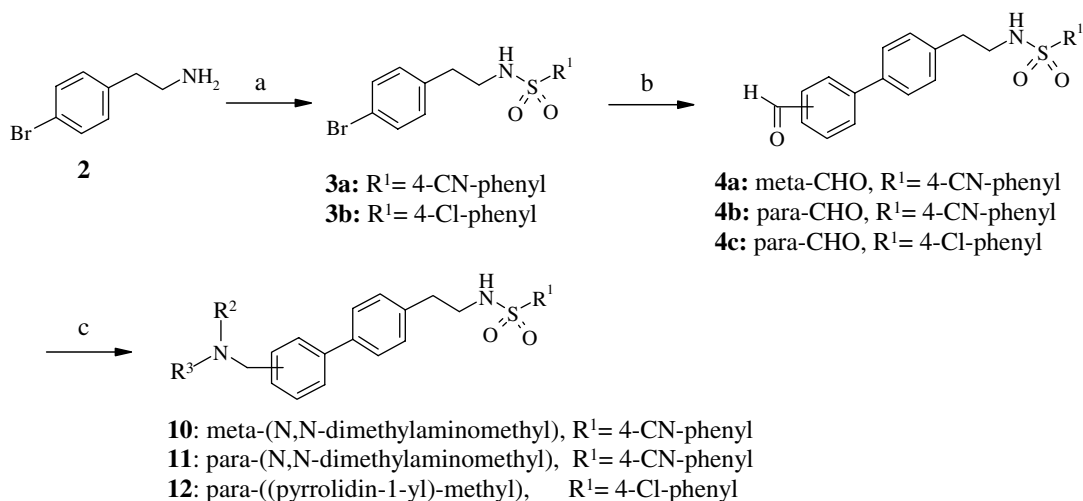
Reductive amination of intermediate **6** with 4-chlorobenzaldehyde led to compound **16** (Scheme 4).

The pyrazole derivative **24** was obtained by the treatment of the acetyl intermediate **9a** with DMF dimethylacetal, followed by cyclization with hydrazine hydrate (Scheme 5).

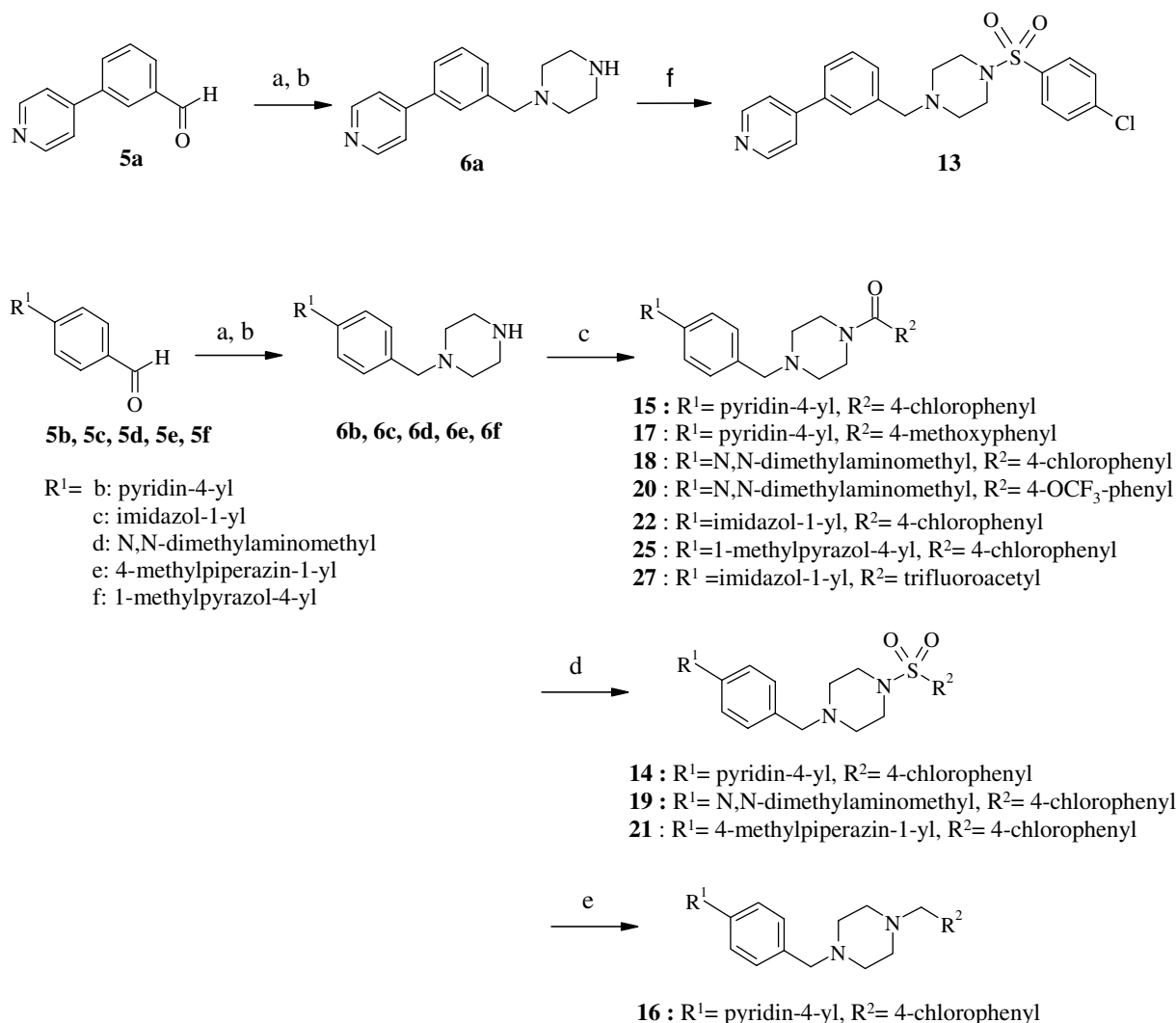
The oxadiazole derivative **26** was obtained by the treatment of the cyano intermediate **9b** with hydroxylamine hydrochloride, followed by cyclization of the resulting amidoxime with acetic anhydride (Scheme 5).

2.3. Lead optimization

A lead optimization process was conducted starting from compound **1**. All compounds meeting an in vitro potency threshold (IC₅₀ less than 50 nM) were evaluated in vivo in the rat at a single dose of 2 mg/kg, monitoring inhibition of cholesterol synthesis in both liver and lens. In parallel, the appearance of MonoEpoxySqualene (MES) as a marker of OSC inhibition was evaluated in



Scheme 3. Reagents and conditions: (a) R¹SO₂Cl, Et₃N, CH₂Cl₂, rt; (b) 3- or 4-formyl-phenyl boronic acid, Pd(PPh₃)₄, LiCl, Na₂CO₃, toluene, reflux; (c) R²R³NH, NaHB(OAc)₃, CH₂Cl₂, rt.



Scheme 4. Reagents and conditions: (a) *N*-Boc-piperazine, NaHB(OAc)₃, CH₂Cl₂, rt; (b) CF₃COOH, CH₂Cl₂, rt; (c) R²-COCl, NEt₃, CH₂Cl₂, rt; or R²-CO-O-CO-R², NEt₃, CH₂Cl₂, rt, or R²-COOH, HOBT, EDCI, NEt₃, DMF, rt; (d) R²-SO₂Cl, NEt₃, CH₂Cl₂, rt; (e) R²-CHO, NaHB(OAc)₃, CH₂Cl₂, rt; (f) 4-chlorophenyl-SO₂Cl, NEt₃, CH₂Cl₂, rt.

the same organs (inhibition of OSC leads to the inhibition of the production of cholesterol and to the accumulation of 2,3 mono-epoxysqualene).

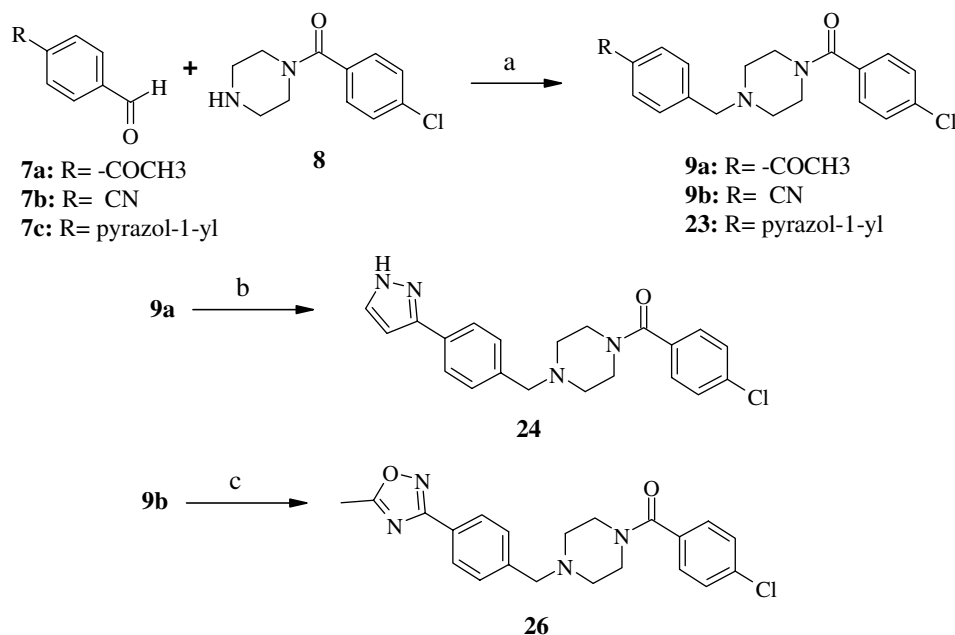
Compound **1** was selected as a starting point for medicinal chemistry, because of its high chemical tractability and its good in vitro activity, and even if it was devoid of any in vivo activity at 2 mg/kg (data not shown). Chemical modifications depicted in Scheme 6 were undertaken in order to obtain compounds, with in vitro potency and in vivo activity comparable to inhibitors reported earlier in the literature.

Replacement of the pyridin-3-yl-hydroxymethylene group by a *para*-dialkylaminophenyl gave potent OSCi (compounds **11** and **12**) (Table 1). Comparison with the inactive analogue **10**, containing the *meta*-dialkylaminophenyl, showed the importance of an extended conformation as expected with the *para* substitution. Compound **11** was tested in vivo, but was poorly active probably due to metabolic instability (high rat microsomal clearance) (Table 3).

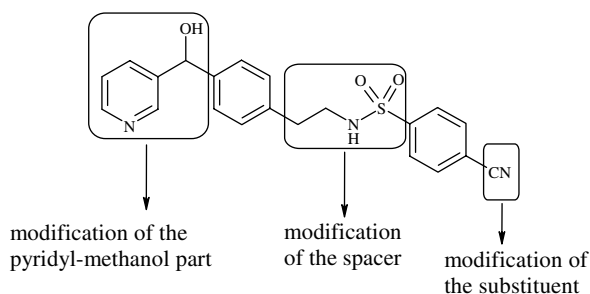
The hydroxymethylene spacer was then removed and the ethylamino spacer was rigidified (Table 2). In order to maintain an adequate distance between extremity features required by the pharmacophore model, compound **14** was prepared and was highly potent in vitro. Once again, the meta analogue (compound **13**) showed a drop in potency.

On the right side of the molecule, the sulfonamide function can be replaced by an amide function (compound **15**), but the corresponding aminomethyl compound (compound **16**) was 100-fold less potent, showing the importance of an H-bond acceptor in this part of the molecule. An aromatic ring is crucial for in vitro activity (compound **27**), and an electron-withdrawing substituent in the *para* position of this aromatic ring is important for potency (compound **17**).

As pyridine analogues (compounds **14** and **15**) gave moderate in vivo activity in the rat (Table 3), further optimization of the left side of the molecule was conducted.



Scheme 5. Reagents and conditions: (a) NaHB(OAc)₃, CH₂Cl₂, rt; (b) i:DMF·DMA, reflux; ii:H₂N-NH₂·H₂O, EtOH, reflux; (c) i:NH₂OH·HCl, AcONa, EtOH/H₂O, reflux; ii:(CH₃CO)₂O, NEt₃, CH₂Cl₂, rt.



Scheme 6. Chemical modifications performed on compound **1**.

The replacement of the pyridine by dialkyl amino groups such as *N,N*-dimethylaminomethyl (compounds **18–20**) or a *N*-methylpiperazine (compound **21**), maintained in vitro potency. The replacement of the pyridine by an imidazole gave the potent analogue **22**. In vivo, compound **19** showed an improved inhibition of cholesterol synthesis but a moderate apparition of MES synthesis whereas compounds **20–22** led to a great

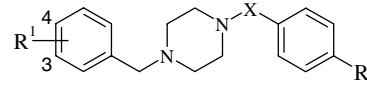
improvement of in vivo activity (Table 3), comparable with **BIBB 515**.

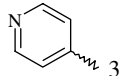
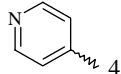
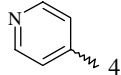
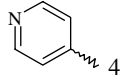
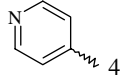
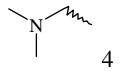
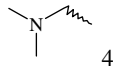
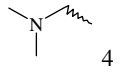
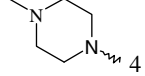
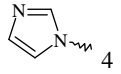
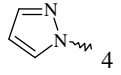
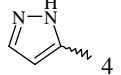
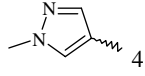
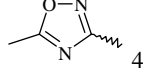
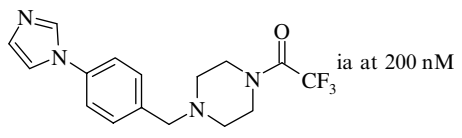
Replacement of the imidazole by a pyrazole or an oxadiazole (compounds **23–26**) led to a dramatic loss of potency. As suggested by our pharmacophore model, one of the heteroatoms of these heterocycles is expected to give a hydrogen-bond, mimicking the basic nitrogen of RO48-8071 as shown in Figure 1. This interaction was confirmed by X-ray observations, as the basic nitrogen of RO48-8071 is shown to be hydrogen-bonded with the carboxylic acid of Asp455.²⁰ Moreover, X-ray data showed that this terminal part of RO48-8071 is located into a quite small and mainly hydrophobic pocket, apart from Asp455.²⁰ Although our pharmacophore model is not precise enough to explain the loss of potency of compounds **23–26**, we can assume from X-ray observations that a sub-optimal orientation of an hydrogen-bond donor atom of the heterocycle would prevent it from forming the hydrogen-bond with Asp455. In addition, an unfavorable interaction of an heterocycle sub-

Table 1. Effect of replacement of the pyridin-3-yl-hydroxymethylene group of compound **1** on OSC inhibition

Compound	R ¹	R ²	OSC inhibition IC ₅₀ (nM)
10	3-[(<i>N,N</i> -Dimethylamino) methyl]	CN	ia at 200 nM
11	4-[(<i>N,N</i> -Dimethylamino) methyl]	CN	28
12	4-[(Pyrrolidin-1-yl) methyl]	Cl	63

ia at 200 nM, inactive at 200 nM.

Table 2. Effect of replacement of the pyridin-3-yl-hydroxymethylene group and rigidification of the ethylamino spacer of compound **1** on OSC inhibition


Compound	R ¹	R ²	X	OSC inhibition IC ₅₀ (nM)
13		Cl	–SO ₂ –	500
14		Cl	–SO ₂ –	13
15		Cl	–CO–	3
16		Cl	–CH ₂ –	316
17		–OMe	–CO–	2511
18		Cl	–CO–	40
19		Cl	–SO ₂ –	32
20		–OCF ₃	–CO–	20
21		Cl	–SO ₂ –	6
22		Cl	–CO–	32
23		Cl	–CO–	ia at 200 nM
24		Cl	–CO–	ia at 200 nM
25		Cl	–CO–	ia at 200 nM
26		Cl	–CO–	ia at 200 nM
27				ia at 200 nM

ia at 200 nM, inactive at 200 nM.

stituent (NH, N, and methyl) with a close amino-acid of the hydrophobic pocket would be responsible for the observed biological results for these compounds. Docking experiments in the X-ray crystal structure of OSC would be necessary to prove these hypotheses.

Overall in this study, the observed SAR in our series is coherent with the published SAR of the compounds used for the pharmacophore generation. Three inhibitors with in vivo potency comparable to **BIBB 515** were identified (compounds **20–22**), and their PK profiles and duration of action were determined in rat (Table 4).

Compounds **20** and **21** showed similar profiles in terms of potency and duration of action (similar activity after 8 h) both in liver and lens. After iv administration, both these have a lower exposure in plasma and a much higher exposure in liver than **BIBB 515**. Moreover, compound **21** has high hepatic exposure versus plasma or lenticular exposure, compared to **20**. Interestingly compound **22** showed a significantly different profile in that almost all activity disappeared by 8 h of treatment both in liver and lens. However, **22** also had a lower exposure in plasma and a higher hepatic exposure than **BIBB 515**.

We selected compounds **21** and **22** based on their distinct PK profiles. While both these showed a higher liver/lens and a lower plasma/liver exposure ratio compared to **BIBB 515**, **21** showed a long duration of action associated with the highest liver/lens exposure ratio whereas **22** displayed a short duration of action. Both compounds displayed the same efficacy in vivo at 2 mg/kg and neither demonstrated major pharmacokinetic issues (data not shown).

2.4. Toxicological study

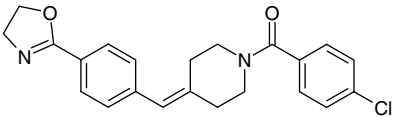
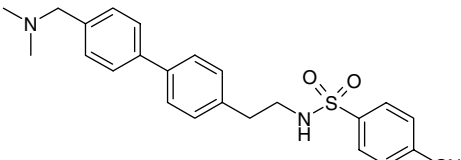
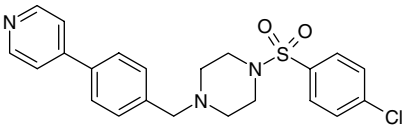
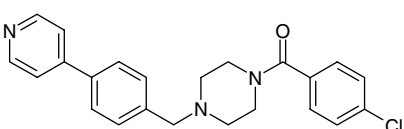
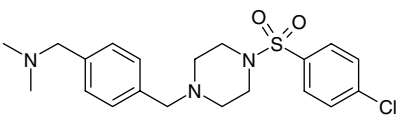
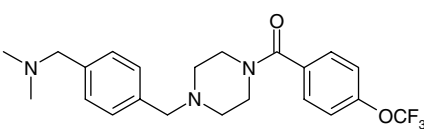
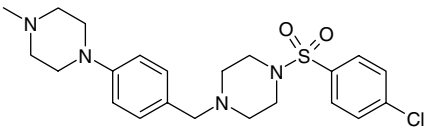
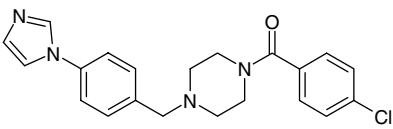
Rats (3 males and 3 females) were treated with compounds **21** and **22** for 21 days;

The compounds were administered po at 2, 10, and 30 mg/kg once a day. On the last day of treatment, plasmatic area under the curves (AUC) was calculated (data not shown). A therapeutic window could thus be evaluated as the ratio of plasmatic AUC calculated at the 1st dose of cataract apparition versus plasmatic AUC calculated at the pharmacological active dose. Histology was performed on lens, liver, and additional organs. Ophthalmology was conducted using the slit-lamp biomicroscope technique. In parallel, activity for OSC inhibition, and drug exposure were monitored.

Noticeably, but as expected from the previously published toxicological data, no relevant findings were observed in the area of hematology, blood chemistry, liver enzymes, macroscopic post-mortem examination, and liver histology for either compound. However, lenticular changes were found.

Compound **21** gave a dose-dependent and very severe cataract phenotype. This adverse effect was detectable at the lowest dose of 2 mg/kg, which is also a pharmacologically active dose. Histological examination of the eye

Table 3. Effects of compounds on hepatic OSC inhibition following single-dose treatment

Compound	Rat microsomes Cl _{int} (mL/min/g)	% Inhibition of cholesterol synthesis in liver	Induction of MES synthesis in liver (% of BIBB B515-treated animals)
 BIBB 515	2.3	85	100
 11	9.9	47	6
 14	1.3	66	45
 15	6	64	55
 19	2.5	74	55
 20	3.6	83	100
 21	5.4	75	111
 22	0.2	85	156

OFA rats were treated for 3 h with compounds at 2 mg/kg po as indicated in Section 4. Inhibition of neosynthesized cholesterol in liver was calculated in comparison with vehicle-treated animals. Induction of neosynthesized MES was expressed as percentage of **BIBB 515**-treated animals used as standard (100%).

revealed a keratosis and degeneration of lenticular fibers. Despite very low exposure in plasma and a high he-

patic exposure, no therapeutic window was achieved with compound **21** (Table 5). For compound **22**, no

Table 4. In vivo profile of compounds **20–22**

Compound	In vivo lipid synthesis after 3 h		In vivo lipid synthesis after 8 h		AUC _{0–6 h} , ng H/mL (1 mg/kg, iv bolus)	Tissular exposure (1 mg/kg, iv)	
	Liver Chol/MES	Lens Chol/MES	Liver Chol/MES	Lens Chol/MES		Liver (ng/g)	Eyes (ng/g)
BIBB 515	92/100	79/100	40/100	61/100	1027 ± 72 ^a	C _{2h} = 301 ± 53 ^a C _{6h} = 169 ± 49 ^a	C _{2h} < 10 C _{6h} < 10
20	85/112	64/175	69/241	66/51	318; 362 ^b	C _{2h} = 1882; 2416 ^b C _{6h} = 968; 1317 ^b	C _{2h} = 230; 260 ^b C _{6h} = 189; 194 ^b
21	87/94	67/162	62/232	67/29	95; 97 ^b	C _{2h} = 5937; 6605 ^b C _{6h} = 2649; 3272 ^b	C _{2h} = 181; 278 ^b C _{6h} = 83; 123 ^b
22	82/135	76/104	20/85	0/51	504; 534 ^b	C _{2h} = 1999; 2013 ^b C _{6h} = 585; 660 ^b	C _{2h} = 56; 65 ^b C _{6h} < 10

OFA rats were treated for 3 or 8 h with compounds at 2 mg/kg po as indicated in Section 4. At the end of the labeling period, neosynthesized lipids were extracted from liver and lens. Inhibition of neosynthesized cholesterol was calculated in comparison with vehicle-treated animals. Induction of neosynthesized MES was expressed as percentage of level of **BIBB 515**-treated animals used as standard (100%). In parallel, a pharmacokinetic study was performed in rats at 1 mg/kg following intravenous bolus administration, for the determination of plasmatic area under the curves from 0 to 6 h (AUC_{0–6h}) and tissue exposures.

^a Means ± SD, six independent experiments.

^b Values from two independent experiments.

Table 5. Toxicological study in rats

Compound	Proof of activity MES appearance in liver		Opacification of the anterior lens scoring from 0 to 6 ^a	
Control	M	–	0/0/0	—
	F	–	0/0/0	—
21				
2 mg/kg	M	+	0/1/4	Very slight/slight
	F	+	1/1/2	
10 mg/kg	M	+	1/1/3	Moderate
	F	+	4/4/4	
30 mg/kg	M	+	4/4/6	Marked/very marked
	F	+	3/4/6	
22				
2 mg/kg	M	–	0/0/0	Nothing
	F	+	0/0/0	
10 mg/kg	M	+	1/2/3	Slight/moderate
	F	+	3/3/3	
30 mg/kg	M	+	4/4/5	Very marked
	F	+	4/5/6	

Sprague–Dawley rats (male and female $n = 3$) were treated for 21 days, orally once a day, with increasing doses of compounds **21** and **22**. At the end of the treatment, lipids were extracted from the liver and MES appearance was evaluated as proof of drug activity. Opacification of the anterior lens was determined and scored between 0 (no abnormalities) to 6 (severe findings).

^a 0, no abnormalities; 1, very slight; 2, slight; 3, moderate; 4, marked; 5, very marked; 6, severe.

abnormalities were detected at 2 mg/kg. In males at 2 mg/kg, surprisingly no OSC inhibition was observed, but in females, this dose was pharmacologically active. At the highest dose a very marked cataract phenotype was observed. Interestingly, only slight keratosis and moderate degeneration of lenticular fibers appeared at the intermediate dose of 10 mg/kg (Table 5) for which the plasma exposure of **22** was 7- to 12-fold higher than that seen following the 2 mg dose (data not shown). Therefore, the low plasma/liver exposure ratio combined with the short duration of action of compound **22**, led to no observable abnormalities in lens at the pharmacolog-

ical dose of 2 mg/kg. Nevertheless, despite an improved toxicological profile compared to **21**, the therapeutic window appears very limited (<10) for such a severe finding and confirmation in higher species would be required before any further development of the compound.

3. Conclusion

The aim of this work was to test the hypothesis that the cataractogenic potential of an OSCi could be managed by a decrease in systemic exposure. With that goal in mind, we undertook a pharmacophore-based focused screen and discovered compound **1** as a novel and tractable OSCi. We optimized this series to select two compounds (**21** and **22**) displaying good in vitro and in vivo potency and distinct pharmacokinetic profiles with reduced systemic exposure as compared to **BIBB 515**. We have demonstrated with compound **21** that a very low systemic exposure is not sufficient to remove the ocular side effects. Compound **22** which displayed a low systemic exposure combined with a short duration of action showed a somewhat improved therapeutic window. However, it is not clear that this small improvement is sufficient to enable the liabilities of OSCi to be adequately managed. These results, in addition to previously published toxicological data, suggest that the development of an OSCi for the treatment of dyslipidemia free of ocular toxicity remains high-risk.

4. Experimental

4.1. Sterol synthesis in HepG2 cells

2,3-oxidosqualene cyclase activity was determined in the human hepatoma cell line, HepG2, by measuring the inhibition of [¹⁴C]cholesterol synthesis concomitantly with the formation of [¹⁴C]2,3-mono-epoxy-squalene (MES) and [¹⁴C]2,3,22,23-diepoxy-squalene (DES).

Cells plated in 96-well plates, were incubated for 24 h in the absence (control) or presence of compounds in BME medium containing 10% of fetal calf serum and then labeled with 7.4 kBq of [^{14}C]mevalonate (Perkin-Elmer). At the end of the incubation, lipids were extracted with heptane/isopropanol (99:1, v/v) and separated by thin-layer chromatography using cyclohexane/ethylacetate (90:10, v/v). [^{14}C]cholesterol, MES, and DES were identified using purified standards and the radioactivity associated with each individual lipid was quantified using a Phosphoscreen (Strom, Molecular Dynamics).

Data are expressed as percentage of control for cholesterol synthesis inhibition.

Reference compound, **BIBB 515**, showed an IC_{50} of $0.00585 \pm 0.0034 \mu\text{M}$ (33 measurements).

4.2. Sterol synthesis in rat

For single-dose treatment, OSC activity was determined in rat by measuring the inhibition of [^{14}C]cholesterol synthesis concomitantly with the formation of [^{14}C]2,3-mono-epoxysqualene (MES) and [^{14}C]2,3;22,23-diepoxysqualene (DES).

Male OFA rats were orally treated with compounds at the indicated doses for 2 h. Cholesterol and MES synthesis were assessed by intraperitoneal injection of 370 kBq of [^{14}C]mevalonate for an additional hour. After sacrifice, liver and lens were removed and lipids were extracted using isopropanol and separated by thin-layer chromatography as above. [^{14}C]Cholesterol, MES, and DES were identified using purified standards and the radioactivity associated with each individual lipid was quantified using a Phosphoscreen (Strom, Molecular Dynamics). Data are expressed as percentage of control for cholesterol synthesis inhibition.

For toxicological study, OSC activity was determined in rat by measuring the formation of MES. On day 21, 3 h after last administration, animals were sacrificed and hepatic lipids were extracted and analyzed as described above. MES formation was assessed by staining the thin-layer chromatography with 5% phosphomolybdic acid in isopropanol in order to visualize the different lipids. Quantification of MES mass was done using a densitometer (PDSI, Molecular Dynamics).

4.3. Metabolic stability of OSC inhibitors in pooled rat-liver microsomal incubations

Pooled rat-liver microsomes (Xenotech, Lenexa, KA) were diluted in Tris buffer 0.1 M, pH 7.4, containing 10 mM MgCl_2 . The incubation mixtures (1.5 mL total volume), which contained 0.5 mg/mL of microsomal proteins and 1.25 $\mu\text{g/mL}$ of OSC inhibitors, were preincubated for 5 min at 37 °C. The reactions were initiated by addition of NADPH (final 0.48 mM), continued for 30 min, and stopped by the addition of 1 volume of cold acetonitrile. Incubates were then centrifuged for 15 min at 4000 rpm and 50 μL of the supernatant was injected into the chromatographic system. Chromatographic

separations were performed on a supelcosil LC ABZ⁺ column (150 \times 4.6 mm, 5 μm) under two solvent gradient conditions at 30 °C with a flow rate of 1 mL/min and UV detection at 290 nm. Mobile phases consisted of 50 mM ammonium acetate (A) and acetonitrile (B). The results were expressed as intrinsic clearances (Cl_{int} , mL/min/g), assuming 45 mg of microsomal proteins per gram liver.

4.4. Pharmacokinetics and tissue exposure

OSC inhibitors were administered to OFA rats ($n = 10$) by intravenous injection via the penis vein at a dose of 1 mg/kg in 10% DMA and 90% PEG200. Blood samples were collected at T_5 , T_{30} , T_{120} , T_{240} , and T_{360} (min). Tissues (liver and the 2 eyes) were collected at selected times (T_{120} and T_{360}). Plasma samples (0.5 mL) were diluted with 1:1 borate buffer (0.1 M, pH 11.5) and then extracted with ethyl ether (4 mL). The ethyl ether was evaporated and the residues resuspended in 300 μL of mobile phase (water/acetonitrile, 40:60, v/v, ammonium acetate 5 mM). Liver samples (1 g) and eyes were homogenized in borate buffer 0.1 M, pH 11.5 (3 and 1.5 mL, for liver and eyes, respectively). The homogenates were centrifuged at 4000 rpm for 15 min at 4 °C. The liver (1 mL) and the eye (0.5 mL) homogenates were diluted with 1:1 borate buffer (0.1 M, pH 11.5) and then extracted with ethyl ether (4 mL). The ethyl ether was evaporated and the residues resuspended in 1 mL and 300 μL of mobile phase (water/acetonitrile, 40:60, v/v, ammonium acetate 5 mM), for liver and eye extracts, respectively. Samples were analyzed by high-performance liquid chromatography coupled to tandem mass spectrometry (LC/MS/MS). Chromatographic separations were performed on a supelcosil LC ABZ⁺ column (150 \times 2.1 mm, 5 μm) under two solvent gradient conditions at 30 °C with a flow rate of 0.2 mL/min. Mobile phases consisted of water (A) and acetonitrile (B), both containing 5 mM ammonium acetate, and 20 μL was injected into the chromatographic system. The mass spectrometer was a Quattro Ultima (Waters), operated in the positive ion mode. The MS/MS detection was carried out by using the multiple monitoring reaction mode. The areas under the curve (AUC) were obtained from SIPHAR (Simed).

4.5. Pharmacophore generation

Molecular modeling studies were performed using Catalyst4.5 (Accelrys) installed on a Silicon Graphics Octane2 workstation. Conformations were calculated using an energy cutoff of 15 kcal with the best option. The number of conformers generated for each molecule was limited to a maximum of 250. Pharmacophore hypothesis was generated with the common features algorithm. The database search was conducted with the best option.

4.6. Chemistry

All starting materials were commercially available and used without further purification. All reactions were carried out with the use of standard techniques under an

inert atmosphere (Ar or N₂). Organic extracts were routinely dried over anhydrous sodium sulfate. Solvent removal refers to rotary evaporation under reduced pressure at 30–40 °C. The analytical thin-layer chromatography (TLC) was carried out on E. Merck 60-F₂₅₄ precoated silica gel plates and components were usually visualized using UV light, iodine vapor, or Dragendorff preparation. Flash column chromatography was performed using silica gel, Merck grade 60 (230–400 mesh). Melting points were determined on a hot-stage Kofler apparatus and are uncorrected. Proton NMR (¹H NMR) spectra were recorded at ambient temperature on Bruker Avance 300 DPX spectrometers using tetramethylsilane as internal standard and proton chemical shifts (δ) are expressed in ppm in the indicated solvent. The following abbreviations are used for multiplicity of NMR signals: s = singlet, d = doublet, t = triplet, q = quadruplet, dd = double doublet, m = multiplet, ddd = doublet of doublet of doublet, and br = broad. Analytical HPLC (method A) was conducted on a X-Terra MS C₁₈ column (2.5 μ m 30 \times 3 mm id) eluting with 0.01 M ammonium acetate in water (solvent A) and 100% acetonitrile (solvent B), using the following elution gradient 0–4 min 0–100%B, 4–5 min 100%B at a flow rate of 1.1 mL/min. The mass spectra were recorded on a micromass Platform-LC mass spectrometer using atmospheric pressure chemical positive ionization [AP+ve to give [M+H]⁺ molecular ions] or atmospheric pressure chemical negative ionization [AP–ve to give [M–H][–] molecular ion] modes (MS-APCI).

Analytical HPLC (method B) was conducted on a X-Bridge C₁₈ column (2.5 μ m 30 \times 3 mm id) eluting with 0.01 M ammonium acetate in water (solvent A) and 100% acetonitrile (solvent B) using the following elution gradient: 0–0.5 min 5% B, 0.5–3.5 min 5% B–100% B, 3.5–4 min 100% B, 4–4.5 min 100% B–5% B, 4.5–5.5 min, 5% B at a flow rate of 1.3 mL/min with a temperature of 40 °C. The mass spectra were recorded on a micromass LCT mass spectrometer using electrospray-positive ionization [ES+ve to give [M+H]⁺ molecular ion] or electrospray-negative ionization [ES–ve to give [M–H][–] molecular ion] modes (HRMS-ESI).

The purity of the compounds was determined on two analytic HPLC systems by UV detection (100% purity in both methods was obtained for the examples described below).

4.6.1. N-[2-(4-Bromophenyl)ethyl]-4-cyanobenzenesulfonamide (3a). To a solution of 4-bromophenethyl amine **2** (Aldrich, 2.5 g, 12.49 mmol) in CH₂Cl₂ (50 mL) were added 4-cyanobenzenesulfonyl chloride (Aldrich, 2.64 g, 13.12 mmol), then triethylamine (2.1 mL, 15 mmol) and the mixture was stirred at room temperature for 30 min and then diluted with CH₂Cl₂ (100 mL). The organic phase was washed with water, dried (Na₂SO₄), and evaporated under reduced pressure to provide **3a** as a colorless oil which crystallized (4.55 g, 99%); mp: 140 °C; ¹H NMR (CDCl₃) δ : 7.79 (d, 2H, 8.67 Hz), 7.69 (d, 2H, 8.67 Hz), 7.29 (d, 2H, 8.48 Hz), 6.88 (d, 2H, 8.29 Hz), 4.63 (t, 1H), 3.18 (q, 2H), and 2.69 (t, 2H).

4.6.2. N-[2-(4-Bromophenyl)ethyl]-4-chlorobenzenesulfonamide (3b). Following the procedure used for **3a**, 4-bromophenethyl amine **2** (5 g, 25 mmol), 4-chlorobenzenesulfonyl chloride (5.54 g, 26.24 mmol) and triethylamine (4.2 mL, 30 mmol) were used to give **3b** as a cream solid (9.34 g, 99%); mp: 118 °C; ¹H NMR (CDCl₃) δ : 7.73 (d, 2H, 8.67 Hz), 7.37 (d, 2H, 8.85 Hz), 7.29 (d, 2H, 8.48 Hz), 6.87 (d, 2H, 8.29 Hz), 4.50 (t, 1H), 3.13 (q, 2H), and 2.67 (t, 2H).

4.6.3. N-[2-(4-(3-Formylphenyl)phenyl)ethyl]-4-cyanobenzenesulfonamide (4a). Intermediate **3a** (1 g, 2.74 mmol) and tetrakis triphenylphosphine palladium[0] (0.159 g, 0.14 mmol) in toluene (50 mL) were stirred under nitrogen at room temperature for 10 min. 3-Formylbenzeneboronic acid (Aldrich, 0.53 g, 3.56 mmol), LiCl (0.35 g, 8.22 mmol), and Na₂CO₃ (3.5 mL of a solution 2 M, 6.84 mmol) were added and the mixture was heated under reflux for 3 h, then cooled, and poured in water. The aqueous phase was extracted twice with CH₂Cl₂ and the organic phase was dried (Na₂SO₄) and evaporated under reduced pressure. The resulting residue was purified by flash chromatography (CH₂Cl₂/MeOH, 99:1 then 98:2) to provide **4a** as a colorless oil (0.52 g, 49%); ¹H NMR (CDCl₃) δ : 10 (s, 1H), 7.99 (s, 1H), 7.84 (d, 2H, 8.48 Hz), 7.77 (m, 2H), 7.69 (d, 2H, 8.48 Hz), 7.55 (t, 1H, 7.54 and 7.72 Hz), 7.46 (d, 2H, 8.10 Hz), 7.12 (d, 2H, 8.29 Hz), 4.70 (t, 1H), 3.25 (q, 2H), and 2.79 (t, 2H).

4.6.4. N-[2-(4-(4-Formylphenyl)phenyl)ethyl]-4-cyanobenzenesulfonamide (4b). Following the procedure used for **4a**, **3a** (2.85 g, 7.81 mmol), tetrakis triphenylphosphine palladium[0] (0.45 g, 0.4 mmol), 4-formylbenzeneboronic acid (Aldrich, 1.52 g, 10.15 mmol), LiCl (1 g, 23.42 mmol), and Na₂CO₃ (10 mL of a solution 2 M, 20 mmol) were used to provide after flash chromatography (CH₂Cl₂ then CH₂Cl₂/MeOH, 98:2), compound **4b** as a white solid (1.8 g, 59%); mp: 174 °C; ¹H NMR (CDCl₃) δ : 10.01 (s, 1H), 7.9 (d, 2H, 8.48 Hz), 7.86 (d, 2H, 8.67 Hz), 7.72 (d, 2H, 8.67 Hz), 7.66 (d, 2H, 8.29 Hz), 7.50 (d, 2H, 8.29 Hz), 7.15 (d, 2H, 8.10 Hz), 4.55 (t, 1H), 3.29 (q, 2H), and 2.83 (t, 2H).

4.6.5. N-[2-(4-(4-Formylphenyl)phenyl)ethyl]-4-chlorobenzenesulfonamide (4c). Following the procedure used for **4a**, **3b** (5 g, 13.35 mmol), tetrakis triphenylphosphine palladium[0] (1.54 g, 1.33 mmol), 4-formylbenzeneboronic acid (Aldrich, 2.6 g, 17.36 mmol), LiCl (1.7 g, 40 mmol), and Na₂CO₃ (17.2 mL of a solution 2 M, 34.4 mmol) were used to provide after flash chromatography (CH₂Cl₂ then CH₂Cl₂/MeOH, 98:2), compound **4c** as a white solid (3.8 g, 71%); ¹H NMR (CDCl₃) δ : 9.99 (s, 1H), 7.87 (d, 2H, 8.48 Hz), 7.66 (d, 2H, 8.67 Hz), 7.64 (d, 2H, 8.10 Hz), 7.47 (d, 2H, 8.29 Hz), 7.37 (d, 2H, 8.67 Hz), 7.12 (d, 2H, 8.29 Hz), 4.36 (t, 1H), 3.22 (q, 2H), and 2.78 (t, 2H).

4.6.6. N-[3-(Pyridin-4-yl)phenylmethyl]-piperazine (6a). To a solution of 3-(pyridin-4-yl)-benzaldehyde²¹ (0.8 g, 4.37 mmol) in CH₂Cl₂ (50 mL) were added *N*-tertbutyloxycarbonylpiperazine (Fluka, 0.896 g, 4.81 mmol) and sodium triacetoxyborohydride (1.11 g, 5.24 mmol) and

the mixture was stirred at room temperature overnight. The reaction was diluted with CH_2Cl_2 (100 mL), washed with water, and the organic phase was dried (Na_2SO_4), and evaporated under reduced pressure. The residue was purified by flash chromatography on silica gel ($\text{CH}_2\text{Cl}_2/\text{MeOH}$, 99:1 then 98:2) to afford 1-(tertbutyloxycarbonyl)-4-[3-(pyridin-4-yl)phenylmethyl]-piperazine as a colorless oil (1.17 g, 76%). ^1H NMR (CDCl_3) δ : 8.64 (d, 2H, 5.84 Hz), 7.60 (s, 1H), 7.52 (m, 3H), 7.44 (t, 1H, 7.35 and 7.72 Hz), 7.39 (d, 1H, and 7.35 Hz), 3.58 (s, 2H), 3.44 (m, 4H), 2.42 (m, 4H), and 1.45 (s, 9H). To a solution of 1-(tertbutyloxycarbonyl)-4-[3-(pyridin-4-yl)phenylmethyl]-piperazine (1.15 g, 3.26 mmol) in CH_2Cl_2 (80 mL) was added dropwise trifluoroacetic acid (5 mL), and the mixture was stirred at room temperature for 3 h, diluted with CH_2Cl_2 (100 mL), and washed with a NaOH solution 1 N, and then with water. The organic phase was dried over Na_2SO_4 and evaporated under reduced pressure to provide **6a** as a colorless oil; (0.8 g, 97%); ^1H NMR (CDCl_3) δ : 8.58 (d, 2H, 6.22 Hz), 7.54 (s, 1H), 7.45 (m, 3H), 7.36 (t, 1H, 7.72 and 6.78 Hz), 7.33 (d, 1H, 7.35 Hz), 3.50 (s, 2H), and 2.83 (m, 4H), 2.38 (m, 4H).

4.6.7. N-[4-(Pyridin-4-yl)phenylmethyl]-piperazine (6b). Following the procedure used for **6a**, 4-(pyridin-4-yl)-benzaldehyde²¹ (1.5 g, 8.2 mmol), *N*-tertbutyloxycarbonylpiperazine (Fluka, 1.6 g, 8.6 mmol) and sodium triacetoxyborohydride (2.08 g, 9.84 mmol) were used to provide 1-(tertbutyloxycarbonyl)-4-[4-(pyridin-4-yl)phenylmethyl]-piperazine as a colorless oil which crystallized on standing (2.86 g, 99%); mp 76–78 °C; ^1H NMR (CDCl_3) δ : 8.56 (d, 2H, 6.22 Hz), 7.51 (d, 2H, 8.29 Hz), 7.43 (d, 2H, 6.03 Hz), 7.35 (d, 2H, 8.10 Hz), 3.49 (s, 2H), 3.37 (t, 4H), 2.35 (t, 4H), and 1.38 (s, 9H). Following the procedure used for compound **6a**, 1-(tertbutyloxycarbonyl)-4-[4-(pyridin-4-yl)phenylmethyl]-piperazine (2.86 g, 8.1 mmol) was hydrolyzed with trifluoroacetic acid (10 mL) to provide **6b** as a white amorphous solid (1.8 g, 88%); ^1H NMR (CDCl_3) δ : 8.61 (d, 2H, 6.22 Hz), 7.56 (d, 2H, 8.29 Hz), 7.47 (d, 2H, 6.22 Hz), 7.41 (d, 2H, 8.10 Hz), 3.53 (s, 2H), 2.91 (t, 4H), 2.45 (m, 4H), and 2.35 (s, 1H).

4.6.8. N-[4-(Imidazol-1-yl)phenylmethyl]-piperazine (6c). Following the procedure used for **6a**, 4-(imidazol-1-yl)-benzaldehyde²² (2.1 g, 12.2 mmol), *N*-tertbutyloxycarbonylpiperazine (Fluka, 2.5 g, 13.42 mmol) and sodium triacetoxyborohydride (2.84 g, 13.42 mmol) were used to provide after flash chromatography ($\text{CH}_2\text{Cl}_2/\text{MeOH}$, 95:5), 1-(tertbutyloxycarbonyl)-4-[4-(imidazol-1-yl)phenylmethyl]-piperazine as a colorless oil (4 g, 96%); ^1H NMR (CDCl_3) δ : 7.83 (s, 1H), 7.36 (d, 2H, 8.48 Hz), 7.26 (d, 2H, 8.48 Hz), 7.2 (br s, 1H), 7.14 (br s, 1H), 3.49 (s, 2H), 3.37 (t, 4H), 2.35 (t, 4H), and 1.38 (s, 9H). Following the procedure used for compound **6a**, 1-(tertbutyloxycarbonyl)-4-[4-(imidazol-1-yl)phenylmethyl]-piperazine (4 g, 11.7 mmol) was hydrolysed with trifluoroacetic acid (15 mL) to provide **6c** as a colorless oil (2.73 g, 96%); ^1H NMR (CDCl_3) δ : 7.85 (s, 1H), 7.43 (d, 2H, 8.48 Hz), 7.33 (d, 2H, 8.48 Hz), 7.28 (br s, 1H), 7.2 (br s, 1H), 3.54 (s, 2H), 2.95 (t, 4H), and 2.47 (m, 5H).

4.6.9. N-[4-(Dimethylaminomethyl)phenylmethyl]-piperazine (6d). Following the procedure used for **6a**, 4-(*N*-dimethylaminomethyl)-benzaldehyde²³ (4.8 g, 29.45 mmol), *N*-tertbutyloxycarbonylpiperazine (Fluka, 6 g, 32.26 mmol), and sodium triacetoxyborohydride (7.5 g, 35.34 mmol) were used to provide 1-(tertbutyloxycarbonyl)-4-[4-(*N*-dimethylaminomethyl)phenylmethyl]-piperazine as a colorless oil; ^1H NMR (CDCl_3) δ : 7.18 (m, 4H), 3.42 (s, 2H), 3.35 (m, 4H), 3.33 (s, 2H), 2.30 (t, 4H), 2.16 (s, 6H), and 1.38 (s, 9H). Following the procedure used for compound **6a**, 1-(tertbutyloxycarbonyl)-4-[4-(*N*-dimethylaminomethyl)phenylmethyl]-piperazine was hydrolyzed with trifluoroacetic acid (50 mL) to provide **6d** as a pale yellow oil (5 g, 73%); ^1H NMR (CDCl_3) δ : 7.02 (m, 4H), 3.24 (s, 2H), 3.16 (s, 2H), 2.64 (t, 4H), 2.17 (m, 4H), and 2 (s, 6H).

4.6.10. N-[4-(4-Methyl-piperazin-1-yl)phenylmethyl]-piperazine (6e). Following the procedure used for **6a**, 4-(4-methyl-piperazin-1-yl)-benzaldehyde²² (3 g, 14.71 mmol), *N*-tertbutyloxycarbonylpiperazine (Fluka, 3.01 g, 16.17 mmol), and sodium triacetoxyborohydride (3.74 g, 17.65 mmol) were used to provide after flash chromatography ($\text{CH}_2\text{Cl}_2/\text{MeOH}$, 95:5 then 90:10), 1-(tertbutyloxycarbonyl)-4-[4-(4-methyl-piperazin-1-yl)phenylmethyl]-piperazine as a yellow oil (5.3 g, 96%); ^1H NMR (CDCl_3) δ : 7.31 (d, 2H, 8.67 Hz), 7.00 (d, 2H, 8.67 Hz), 3.56 (s, 2H), 3.55 (m, 4H), 3.34 (m, 4H), 2.95 (m, 2H), 2.71 (m, 4H), 2.49 (s+m, 5H), 1.59 (s, 9H). Following the procedure used for compound **6a**, 1-(tertbutyloxycarbonyl)-4-[4-(4-methyl-piperazin-1-yl)phenylmethyl]-piperazine (1 g, 2.67 mmol) was hydrolysed with trifluoroacetic acid (5 mL) to provide **6e** as a colorless oil (0.63 g, 86%); ^1H NMR (CDCl_3) δ : 7.11 (d, 2H, 8.67 Hz), 6.79 (d, 2H, 8.67 Hz), 3.34 (s, 2H), 3.13 (t, 4H), 2.81 (t, 4H), 2.50 (t, 4H), 2.33 (m, 4H), and 2.18 (br s, 3H).

4.6.11. N-[4-(1-Methyl-pyrazol-4-yl)phenylmethyl]-piperazine (6f). Following the procedure used for **6a**, 4-(1-methyl-pyrazol-4-yl)-benzaldehyde²² (2 g, 10.75 mmol), *N*-tertbutyloxycarbonylpiperazine (Fluka, 2.20 g, 11.83 mmol) and sodium triacetoxyborohydride (3.42 g, 16.13 mmol) were used to provide 1-(tertbutyloxycarbonyl)-4-[4-(1-methyl-pyrazol-4-yl)phenylmethyl]-piperazine as a white solid (3.8 g, 99%); ^1H NMR (CDCl_3) δ : 7.54 (s, 1H), 7.39 (s, 1H), 7.21 (d, 2H, 8.10 Hz), 7.09 (d, 2H, 8.10 Hz), 3.73 (s, 3H), 3.29 (s, 2H), 3.22 (t, 4H), 2.19 (t, 4H), and 1.24 (s, 9H). Following the procedure used for **6a**, 1-(tertbutyloxycarbonyl)-4-[4-(1-methyl-pyrazol-4-yl)phenylmethyl]-piperazine (3.8 g, 10.67 mmol) was hydrolyzed with trifluoroacetic acid (10 mL) to provide **6f** as a white solid (2.2 g, 80%); ^1H NMR (CDCl_3) δ : 7.67 (s, 1H), 7.52 (s, 1H), 7.34 (d, 2H, 8.10 Hz), 7.23 (d, 2H, 8.10 Hz), 3.87 (s, 3H), 3.41 (s, 2H), 2.82 (t, 4H), and 2.35 (m, 4H).

4.6.12. 1-[4-Chlorobenzoyl]-4-[4-acetylphenylmethyl]-piperazine (9a). To a solution of *N*-(4-chlorobenzoyl)-piperazine **8** (Enamine BB, 1.59 g, 7.08 mmol) in CH_2Cl_2 (50 mL) were added 4-acetyl-benzaldehyde **7a** (Aldrich, 1 g, 6.76 mmol) and then portionwise sodium triacetoxyborohydride (2.15 g, 10.13 mmol). The mixture was stirred

red at room temperature overnight. The reaction was diluted with CH_2Cl_2 (150 mL), washed with water, and the organic phase was dried (Na_2SO_4), and evaporated under reduced pressure. The oily residue was crystallized by trituration with *i*-Pr₂O to provide **9a** as white crystals (1.6 g, 66%); mp: 122 °C; ¹H NMR (CDCl_3) δ : 7.93 (d, 2H, 8.29 Hz), 7.43 (d, 2H, 8.29 Hz), 7.38 and 7.34 (2d, 4H, 8.85 Hz), 3.78 (m, 2H), 3.60 (s, 2H), 3.46 (m, 2H), 2.61 (s, 3H), and 2.47 (br m, 4H).

4.6.13. 1-[4-Chlorobenzoyl]-4-[4-cyanophenylmethyl]-piperazine (9b). Following the procedure used for compound **9a**, *N*-(4-chlorobenzoyl)-piperazine **8** (Enamine BB, 3 g, 13.36 mmol), 4-cyano-benzaldehyde **7b** (Aldrich, 1.75 g, 13.36 mmol) and sodium triacetoxymethylborohydride (4.25 g, 20 mmol) were used to provide, after trituration with *i*-Pr₂O, **9b** as white crystals (3.92 g, 86%); mp: 157 °C; ¹H NMR (CDCl_3) δ : 7.62 (d, 2H, 8.29 Hz), 7.46 (d, 2H, 8.29 Hz), 7.39 (d, 2H, 8.67 Hz), 7.34 (d, 2H, 8.85 Hz), 3.79 (m, 2H), 3.60 (s, 2H), 3.45 (m, 2H), and 2.47 (m, 4H).

4.6.14. N-[2-(4-(3-Dimethylaminomethylphenyl)phenyl)ethyl]-4-cyanobenzenesulfonamide (10). To a solution of **4a** (0.2 g, 0.51 mmol) in CH_2Cl_2 (30 mL) were added dimethylamine (Aldrich, solution 2 M/THF, 0.51 mL, 1 mmol) and then portionwise sodium triacetoxymethylborohydride (0.13 g, 0.61 mmol). The mixture was stirred at room temperature overnight. The organic solution was diluted with CH_2Cl_2 , washed with water, then dried (Na_2SO_4), and evaporated under reduced pressure. The oily residue was purified by flash chromatography ($\text{CH}_2\text{Cl}_2/\text{MeOH}$, 98:2 then 9:1). The resulting oil was crystallized by trituration with *i*-Pr₂O to provide **10** as white crystals (0.14 g, 65%); mp: 97 °C; ¹H NMR (CDCl_3) δ : 7.9 (d, 2H, 8.48 Hz), 7.75 (d, 2H, 8.48 Hz), 7.59 (s, 1H), 7.53 (d, 2H, 8.10 Hz), 7.5 (d, 1H, 7.72 Hz), 7.42 (t, 1H, 7.54 Hz), 7.32 (d, 1H, 7.35 Hz), 7.15 (d, 2H, 8.10 Hz), 4.82 (br s, 1H), 3.59 (s, 2H), 3.32 (t, 2H), 2.85 (t, 2H), and 2.35 (s, 6H); MS-APCI 420.10 [M+H]⁺; HRMS-ESI: calculated for $\text{C}_{24}\text{H}_{25}\text{N}_3\text{O}_2\text{S}_1$ [M+H]⁺ 420.1746, found 420.1783; retention time = 2.64 min.

4.6.15. N-[2-(4-(4-Dimethylaminomethylphenyl)phenyl)ethyl]-4-cyanobenzenesulfonamide (11). Following the procedure used for **10**, **4b** (0.3 g, 0.77 mmol), dimethylamine (Aldrich, 0.77 mL of a solution 2 M in THF, 1.54 mmol) and sodium triacetoxymethylborohydride (0.2 g, 0.92 mmol) were used to provide, after flash chromatography ($\text{CH}_2\text{Cl}_2/\text{MeOH}$, 98:2 then 9:1) and trituration of the resulting oily residue with *i*-Pr₂O, **11** as white crystals (0.215 g, 67%); mp: 174 °C; ¹H NMR ($\text{DMSO}-d_6$) δ : 8.05 (d, 2H, 8.67 Hz), 7.94 (d, 2H, 8.67 Hz), 7.61 (d, 2H, 8.10 Hz), 7.56 (d, 2H, 8.10 Hz), 7.39 (d, 2H, 8.29 Hz), 7.25 (d, 2H, 8.10 Hz), 3.46 (s, 2H), 3.25 (br s, 1H), 3.09 (m, 2H), 2.75 (t, 2H), and 2.21 (s, 6H); MS-APCI 420.1 [M+H]⁺; HRMS-ESI: calculated for $\text{C}_{24}\text{H}_{25}\text{N}_3\text{O}_2\text{S}_1$ [M+H]⁺ 420.1746, found 420.1768; retention time = 2.62 min.

4.6.16. N-[2-(4-(4-(Pyrolidin-1-yl)methyl)phenyl)phenyl]ethyl]-4-chlorobenzenesulfonamide (12). Following the

procedure used for **10**, **4c** (0.25 g, 0.63 mmol), pyrrolidine (Aldrich, 0.13 mL, 1.56 mmol) and sodium triacetoxymethylborohydride (0.16 g, 0.75 mmol) were used to provide, after flash chromatography ($\text{CH}_2\text{Cl}_2/\text{MeOH}$, 98:2 then 93:7) and trituration of the resulting oily residue with *i*-Pr₂O, **12** as white crystals (0.165 g, 58%); mp: 140 °C; ¹H NMR (CDCl_3) δ : 7.68 (d, 2H, 8.67 Hz), 7.47 (m, 4H), 7.42 (d, 2H, 8.10 Hz), 7.39 (d, 2H, 8.67 Hz), 7.09 (d, 2H, 8.10 Hz), 4.52 (br s, 1H), 3.80 (s, 2H), 3.20 (m, 2H), 2.76 (m, 6H), and 1.86 (m, 4H); MS-APCI 455.10 [M+H]⁺; HRMS-ESI: calculated for $\text{C}_{25}\text{H}_{27}\text{Cl}_1\text{N}_2\text{O}_2\text{S}_1$ [M+H]⁺ 455.1560, found 455.1565; retention time = 2.94 min.

4.6.17. 1-[4-Chlorophenylsulfonyl]-4-[3-(pyridin-4-yl)phenylmethyl]-piperazine (13). To a solution of **6a** (0.25 g, 0.99 mmol) in CH_2Cl_2 (30 mL) were added 4-chlorobenzenesulfonyl chloride (Aldrich, 0.219 g, 1.04 mmol) and then triethylamine (0.16 mL, 1.18 mmol). The mixture was stirred at room temperature for 30 min and then diluted with CH_2Cl_2 (50 mL). The organic solution was washed with water, dried (Na_2SO_4), and evaporated under reduced pressure. The residue was purified by flash chromatography ($\text{CH}_2\text{Cl}_2/\text{MeOH}$, 99:1, then 95:5). The resulting oil was crystallized by trituration with *i*-Pr₂O to provide **13** as cream crystals (0.183 g, 43%); mp: 128–130 °C; ¹H NMR (CDCl_3) δ : 8.58 (d, 2H, 6.03 Hz), 7.6 (d, 2H, 8.48 Hz), 7.50 (d, 2H, 5.65 Hz), 7.46 to 7.42 (m, 2H), 7.43 (d, 2H, 8.29 Hz), 7.35 (t, 1H, 7.54 Hz), 7.28 (dd, 1H, 7.54 2.45 Hz), 3.7 (s, 2H), 3.1 (m, 4H), and 2.65 (m, 4H); MS-APCI 428.10 [M+H]⁺; HRMS-ESI: calculated for $\text{C}_{22}\text{H}_{22}\text{Cl}_1\text{N}_3\text{O}_2\text{S}_1$ [M+H]⁺ 428.1199, found 428.1194; retention time = 3.21 min.

4.6.18. 1-[4-Chlorophenylsulfonyl]-4-[4-(pyridin-4-yl)phenylmethyl]-piperazine (14). Following the procedure used for **13**, **6b** (0.3 g, 1.18 mmol), 4-chlorobenzene sulfonyl chloride (Aldrich, 0.262 g, 1.24 mmol) and triethylamine (0.2 mL, 1.42 mmol) were used to provide after flash chromatography ($\text{CH}_2\text{Cl}_2/\text{MeOH}$, 99:1 then 97:3) and trituration of the resulting oil with *i*-Pr₂O, **14** as white crystals (0.345 g, 68%); mp: 136 °C; ¹H NMR (CDCl_3) δ : 8.65 (d, 2H, 6.22 Hz), 7.7 (d, 2H, 8.67 Hz), 7.57 (d, 2H, 8.29 Hz), 7.52 (d, 2H, 8.67 Hz), 7.48 (d, 2H, 6.03 Hz), 7.37 (d, 2H, 8.29 Hz), 3.57 (s, 2H), 3.07 (m, 4H), 2.58 (m, 4H); MS-APCI 428.10 [M+H]⁺; HRMS-ESI: calculated for $\text{C}_{22}\text{H}_{22}\text{Cl}_1\text{N}_3\text{O}_2\text{S}_1$ [M+H]⁺ 428.1199, found 428.1201; retention time = 3.28 min.

4.6.19. 1-[4-Chlorophenylsulfonyl]-4-[4-(dimethylaminomethyl)phenylmethyl]-piperazine (19). Following the procedure used for **13**, **6d** (0.5 g, 2.14 mmol), 4-chlorobenzene sulfonyl chloride (Aldrich, 0.455 g, 2.14 mmol) and triethylamine (0.3 mL, 2.14 mmol) were used to provide **19** as a colorless oil (0.87 g, quantitative); ¹H NMR (CDCl_3) δ : 7.6 (d, 2H, 8.67 Hz), 7.41 (d, 2H, 8.48 Hz), 7.15 (d, 2H, 8.10 Hz), 7.10 (d, 2H, 8.29 Hz), 3.4 (s, 2H), 3.31 (s, 2H), 2.95 (t, 4H), 2.44 (t, 4H), and 2.15 (s, 6H); MS-APCI 408.10 [M+H]⁺; HRMS-ESI: calculated for $\text{C}_{20}\text{H}_{26}\text{Cl}_1\text{N}_3\text{O}_2\text{S}_1$ [M+H]⁺ 408.1512, found 408.1523; retention time = 2.51 min.

4.6.20. 1-[4-Chlorophenylsulfonyl]-4-[4-(4-methylpiperazin-1-yl)phenylmethyl]-piperazine (21). Following the procedure used for **13**, **6e** (8.8 g, 32.12 mmol), 4-chlorobenzene sulfonyl chloride (Aldrich, 7.12 g, 33.72 mmol) and triethylamine (5.36 mL, 38.54 mmol) were used to provide, after flash chromatography ($\text{CH}_2\text{Cl}_2/\text{MeOH}$, 99:1 then 95:5) and trituration of the resulting oil with *i*-Pr₂O, **21** as white crystals (11.92 g, 82%); mp: 155–157 °C; ¹H NMR (CDCl_3) δ : 7.69 (d, 2H, 8.48 Hz), 7.51 (d, 2H, 8.67 Hz), 7.12 (d, 2H, 8.67 Hz), 6.85 (d, 2H, 8.67 Hz), 3.42 (s, 2H), 3.21 (t, 4H), 3.03 (m, 4H), 2.59 (t, 4H), 2.51 (t, 4H), and 2.37 (s, 3H); MS-APCI 449.1 [M+H]⁺; HRMS-ESI: calculated for $\text{C}_{22}\text{H}_{29}\text{Cl}_2\text{N}_4\text{O}_2\text{S}_1$ [M+H]⁺ 449.1778, found 449.1819; retention time = 2.74 min.

4.6.21. 1-[4-Chlorophenylcarbonyl]-4-[4-(pyridin-4-yl)phenylmethyl]-piperazine (15). Following the procedure used for **13**, **6b** (0.3 g, 1.19 mmol), 4-chlorobenzoyl chloride (Aldrich, 0.16 mL, 1.24 mmol) and triethylamine (0.2 mL, 1.42 mmol) were used to provide, after flash chromatography ($\text{CH}_2\text{Cl}_2/\text{MeOH}$, 99:1 then 97:3) and trituration of the resulting oil with *i*-Pr₂O, **15** as white crystals (0.358 g, 77%); mp: 160 °C; ¹H NMR (CDCl_3) δ : 8.66 (d, 2H, 6.03 Hz), 7.61 (d, 2H, 8.10 Hz), 7.51 (d, 2H, 6.22 Hz), 7.45 (d, 2H, 8.10 Hz), 7.38–7.39 (2d, 4H, 8.85 Hz), 3.80 (m, 2H), 3.61 (s, 2H), 3.46 (m, 2H), and 2.5 (m, 4H); MS-APCI 392.20 [M+H]⁺; HRMS-ESI: calculated for $\text{C}_{23}\text{H}_{22}\text{Cl}_2\text{N}_3\text{O}_1$ [M+H]⁺ 392.1530, found 392.1510; retention time = 2.86 min.

4.6.22. 1-[4-Chlorophenylcarbonyl]-4-[4-(imidazol-1-yl)phenylmethyl]-piperazine (22). Following the procedure used for **13**, **6c** (13.4 g, 55.37 mmol), 4-chlorobenzoyl chloride (Aldrich, 7.39 mL, 58.14 mmol) and triethylamine (9.24 mL, 66.45 mmol) were used to provide, after flash chromatography ($\text{CH}_2\text{Cl}_2/\text{MeOH}$, 99:1 then 95:5) and trituration of the resulting oil with *i*-Pr₂O, **22** as cream crystals (11.55, 55%); mp: 148 °C; ¹H NMR (CDCl_3) δ : 8.03 (s, 1H), 7.62 (d, 2H, 8.29 Hz), 7.55 (d, 2H, 8.85 Hz), 7.53 (d, 2H, 9.04 Hz), 7.51 (d, 2H, 8.48 Hz), 7.45 (br s, 1H), 7.38 (br s, 1H), 3.96 (m, 2H), 3.77 (s, 2H), 3.65 (m, 2H), and 2.67 (m, 4H); MS-APCI 381.10 [M+H]⁺; HRMS-ESI: calculated for $\text{C}_{21}\text{H}_{21}\text{Cl}_2\text{N}_4\text{O}_1$ [M+H]⁺ 381.1482, found 381.1506; retention time = 2.50 min.

4.6.23. 1-[4-Chlorophenylcarbonyl]-4-[4-(dimethylamino-methyl)phenylmethyl]-piperazine (18). Following the procedure used for **13**, **6d** (0.23 g, 1 mmol), 4-chlorobenzoyl chloride (Aldrich, 0.13 mL, 1 mmol) and triethylamine (0.16 mL, 1.2 mmol) were used to provide, after flash chromatography ($\text{CH}_2\text{Cl}_2/\text{MeOH}$, 90:10), **18** as colorless oil (0.29 g, 79%); ¹H NMR (CDCl_3) δ : 7.39 (d, 2H, 8.67 Hz), 7.35 (d, 2H, 8.29 Hz), 7.28 (br s, 4H), 3.77 (m, 2H), 3.54 (s, 2H), 3.49 (s, 2H), 3.44 (m, 2H), 2.52 (m, 2H), 2.41 (m, 2H), and 2.27 (s, 6H); MS-APCI 372.2 [M+H]⁺; HRMS-ESI: calculated for $\text{C}_{21}\text{H}_{26}\text{Cl}_2\text{N}_3\text{O}_1$ [M+H]⁺ 372.1843, found 372.1866; retention time = 2.35 min.

4.6.24. 1-[4-Chlorophenylcarbonyl]-4-[4-(1-methyl-pyrazol-4-yl)phenylmethyl]-piperazine (25). Following the

procedure used for **13**, **6f** (0.3 g, 1.17 mmol), 4-chlorobenzoyl chloride (Aldrich, 0.156 mL, 1.23 mmol) and triethylamine (0.2 mL, 1.41 mmol) were used to provide, after flash chromatography ($\text{CH}_2\text{Cl}_2/\text{MeOH}$, 99:1 then 95:5) and trituration of the resulting oil with *i*-Pr₂O, **25** as white crystals (0.42 g, 91%); mp: 241 °C; ¹H NMR (CDCl_3) δ : 7.97 (s, 1H), 7.82 (s, 1H), 7.65 (d, 2H, 8.29 Hz), 7.6 (d, 2H, 8.10 Hz), 7.57 (d, 2H, 8.85 Hz), 7.52 (d, 2H, 8.10 Hz), 4.17 (s, 3H), 3.99 (m, 2H), 3.76 (s, 2H), 3.66 (m, 2H), 2.74, and 2.65 (2m, 4H); MS-APCI 395.1 [M+H]⁺; HRMS-ESI: calculated for $\text{C}_{22}\text{H}_{23}\text{Cl}_2\text{N}_4\text{O}_1$ [M+H]⁺ 395.1638, found 395.1655; retention time = 2.63 min.

4.6.25. 1-[4-Methoxyphenylcarbonyl]-4-[4-(pyridin-4-yl)phenylmethyl]-piperazine (17). To a solution of **6b** (0.25 g, 0.99 mmol) in DMF (30 mL) were added 4-methoxybenzoic acid (Aldrich, 0.18 g, 1.18 mmol), HOBT (0.16 g, 1.18 mmol), EDCI (0.227 g, 1.18 mmol), and triethylamine (0.16 mL, 1.18 mmol) and the mixture was stirred at room temperature overnight and then diluted with CH_2Cl_2 . The organic solution was washed with a NaOH solution 1 N, then water, dried (Na_2SO_4), and evaporated under reduced pressure. The residue was purified by flash chromatography ($\text{CH}_2\text{Cl}_2/\text{MeOH}$, 95:5). The resulting oil was crystallized by trituration with *i*-Pr₂O to provide **17** as white crystals (0.26 g, 68%); mp: 162 °C; ¹H NMR (CDCl_3) δ : 8.57 (d, 2H, 6.03 Hz), 7.52 (d, 2H, 8.29 Hz), 7.42 (d, 2H, 6.03 Hz), 7.36 (d, 2H, 8.29 Hz), 7.30 (d, 2H, 8.85 Hz), 6.82 (d, 2H, 8.85 Hz), 3.76 (s, 3H), 3.52 (s, 2H), 2.42 (m, 4H), and 1.61 (m, 4H); MS-APCI 388.2 [M+H]⁺; HRMS-ESI: calculated for $\text{C}_{24}\text{H}_{25}\text{N}_3\text{O}_2$ [M+H]⁺ 388.2025, found 388.2049; retention time = 2.58 min.

4.6.26. 1-[4-(Trifluoromethoxy)phenylcarbonyl]-4-[4-(dimethylaminomethyl)phenylmethyl]-piperazine (20). Following the procedure used for **17**, **6d** (0.23 g, 1 mmol), 4-trifluoromethoxybenzoic acid (Aldrich, 0.226 g, 1.1 mmol), HOBT (0.148 g, 1.1 mmol), EDCI (0.21 g, 1.1 mmol), and triethylamine (0.15 mL, 1.1 mmol) were used to provide, after flash chromatography ($\text{CH}_2\text{Cl}_2/\text{MeOH}$, 9:1), **20** as a colorless oil (0.16 g, 38%); ¹H NMR (CDCl_3) δ : 7.68 (d, 2H, 8.48 Hz), 7.51 (br s, 4H), 7.49 (d, 2H), 4.02 (m, 2H), 3.77 (s, 2H), 3.67 (m, 4H), 2.76 (m, 2H), 2.64 (m, 2H), and 2.49 (s, 6H); MS-APCI 422.2 [M+H]⁺; HRMS-ESI: calculated for $\text{C}_{22}\text{H}_{26}\text{F}_3\text{N}_3\text{O}_2$ [M+H]⁺ 422.2055, found 422.2074; retention time = 2.53 min.

4.6.27. 1-[4-Trifluoroacetyl]-4-[4-(imidazol-1-yl)phenylmethyl]-piperazine (27). To a solution of **6c** (0.2 g, 0.83 mmol) in CH_2Cl_2 (30 mL) were added trifluoroacetic anhydride (Aldrich, 0.17 mL, 1.24 mmol) and then triethylamine (0.14 mL, 1 mmol) and the mixture was stirred at room temperature overnight and then diluted with CH_2Cl_2 . The organic solution was washed with a solution of NaOH 1 N, then water, dried (Na_2SO_4), and concentrated under reduced pressure. The residue was purified by flash chromatography ($\text{CH}_2\text{Cl}_2/\text{MeOH}$, 98:2, then 95:5) to provide **27** as a cream oil (0.19 g, 68%); ¹H NMR (CDCl_3) δ : 7.85 (s, 1H), 7.37 (d, 2H, 8.67 Hz), 7.29 (d, 2H, 8.48 Hz), 7.22 (br s, 1H), 7.16

(br s, 1H), 3.64 (t, 2H), 3.56 (t, 2H), 3.52 (s, 2H), and 2.46 (t, 4H); MS-APCI 243.20 [(M–COCF₃)+H]⁺.

4.6.28. 1-[4-Chlorobenzyl]-4-[4-(pyridin-4-yl)phenylmethyl]-piperazine (16). To a solution of **6b** (0.25 g, 0.99 mmol) in CH₂Cl₂ (30 mL) were added 4-chlorobenzaldehyde (Aldrich, 0.139 g, 0.99 mmol) and then portionwise sodium triacetoxyborohydride (0.31 g, 1.48 mmol). The mixture was stirred at room temperature overnight. The organic solution was diluted with CH₂Cl₂, washed with water, then dried (Na₂SO₄), and evaporated under reduced pressure. The oily residue was purified by flash chromatography (CH₂Cl₂/MeOH, 97:3 then 93:7). The resulting oil was crystallized by trituration with *i*-Pr₂O to provide **16** as white crystals (0.23 g, 58%); mp: 130 °C; ¹H NMR (CDCl₃) δ: 8.65 (d, 2H, 6.22 Hz), 7.59 (d, 2H, 8.29 Hz), 7.51 (d, 2H, 6.22 Hz), 7.44 (d, 2H, 8.29 Hz), 7.28 (br s, 4H), 3.58 (s, 2H), 3.49 (s, 2H), and 2.51 (m, 8H); MS-APCI 378.20 [M+H]⁺; HRMS-ESI: calculated for C₂₃H₂₄ClN₃ [M+H]⁺ 378.1737, found 378.1758; retention time = 3.52 min.

4.6.29. 1-[4-Chlorophenylcarbonyl]-4-[4-(pyrazol-1-yl)phenylmethyl]-piperazine (23). To a solution of 4-(pyrazol-1-yl)benzaldehyde²² (0.3 g, 1.74 mmol) in CH₂Cl₂ (30 mL) were added *N*-(4-chlorobenzoyl)-piperazine **8** (0.43 g, 1.92 mmol) and then portionwise sodium triacetoxyborohydride (0.55 g, 2.62 mmol). The mixture was stirred at room temperature overnight. The organic solution was diluted with CH₂Cl₂, washed with water, then dried (Na₂SO₄), and evaporated under reduced pressure. The oily residue was purified by flash chromatography (CH₂Cl₂/MeOH, 99:1, then 95:5). The resulting oil was crystallized by trituration with *i*-Pr₂O to provide **23** as white crystals (0.35 g, 53%); mp: 149 °C; ¹H NMR (CDCl₃) δ: 7.91 (d, 1H, 2.26 Hz), 7.72 (d, 1H, 1.51 Hz), 7.64 (d, 2H, 8.48 Hz), 7.40 (d, 2H, 8.48 Hz), 7.38 (d, 2H, 8.85 Hz), 7.33 (d, 2H, 8.85 Hz), 6.46 (t, 1H, 2.07 Hz), 3.78 (m, 2H), 3.56 (s, 2H), 3.43 (m, 2H), 2.52, and 2.41 (2m, 4H); MS-APCI 381.1 [M+H]⁺; HRMS-ESI: calculated for C₂₁H₂₁ClN₄O₁ [M+H]⁺ 381.1482, found 381.1526; retention time = 2.76 min.

4.6.30. 1-[4-Chlorophenylcarbonyl]-4-[4-(pyrazol-3-yl)phenylmethyl]-piperazine (24). A solution of intermediate **9a** (1 g, 2.8 mmol) in DMF dimethylacetal (20 mL) was heated under reflux overnight then cooled, and evaporated under reduced pressure. The resulting residue was dissolved in EtOH (30 mL) and then hydrazine hydrate (0.2 mL, 4.13 mmol) was slowly added and the mixture was heated under reflux for 4 h and then poured in to water. The aqueous phase was extracted twice with CH₂Cl₂ and the organic phase was dried (Na₂SO₄) and evaporated under reduced pressure. The crude product was purified by flash chromatography (CH₂Cl₂/MeOH, 95:5 then 90:10) to provide **24** as a cream solid (0.7 g; 89%); mp: 96 °C; ¹H NMR (CDCl₃) δ: 7.59 (d, 2H, 8.10 Hz), 7.49 (d, 1H, 2.26 Hz), 7.26 (d, 2H, 8.85 Hz), 7.24 (d, 2H, 7.54 Hz), 7.22 (d, 2H, 8.85 Hz), 6.49 (d, 1H, 2.26 Hz), 3.66 (m, 2H), 3.45 (s, 2H), 3.32 (m, 2H), 2.41, and 2.32 (2m, 4H); MS-APCI 381.1 [M+H]⁺;

HRMS-ESI: calculated for C₂₁H₂₁ClN₄O₁ [M+H]⁺ 381.1482, found 381.1493; retention time = 2.49 min.

4.6.31. 1-[4-Chlorophenylcarbonyl]-4-[4-(5-methyl-1,2,4-oxadiazol-3-yl)phenylmethyl]-piperazine (26). A mixture of **9b** (1 g, 2.94 mmol), hydroxylamine hydrochloride (Aldrich, 0.33 g, 4.71 mmol) and sodium acetate (0.725 g, 8.84 mmol) in EtOH (50 mL) and water (10 mL) was heated under reflux overnight and then poured in to water. The aqueous phase was extracted twice with CH₂Cl₂ and the organic phase was dried (Na₂SO₄) and evaporated under reduced pressure to provide, after trituration with *i*-Pr₂O of the oily residue, the amidoxime intermediate as a white solid (0.7 g, 64%). The amidoxime intermediate (0.25 g, 0.67 mmol) was dissolved in CH₂Cl₂ (20 mL). Acetic anhydride (0.13 mL, 1.34 mmol) and then triethylamine (0.11 mL, 0.8 mmol) were slowly added and the mixture was stirred at room temperature for 1 h and then under reflux overnight. After cooling, the mixture was poured in to water and neutralized with a saturated NaHCO₃ solution. The aqueous phase was extracted twice with CH₂Cl₂ and the organic phase was dried (Na₂SO₄) and evaporated under reduced pressure. The crude product was purified by flash chromatography (CH₂Cl₂/MeOH, 97:3). The resulting oily residue was trituated with *i*-Pr₂O to provide **26** as white crystals (95 mg, 36%); mp: 142 °C; ¹H NMR (CDCl₃) δ: 7.94 (d, 2H, 8.29 Hz), 7.36 (d, 2H, 8.10 Hz), 7.31 (d, 2H, 8.10 Hz), 7.27 (d, 2H, 8.10 Hz), 3.71 (m, 2H), 3.53 (s, 2H), 3.37 (m, 2H), 2.58 (s, 3H), 2.44 and 2.36 (m, 4H); MS-APCI 397.1 [M+H]⁺; HRMS-ESI: calculated for C₂₁H₂₁ClN₄O₂ [M+H]⁺ 397.1431, found 397.1429; retention time = 2.80 min.

Acknowledgment

The authors acknowledge Dr. Andrew Brewster for helpful discussions and comments on the manuscript.

References and notes

- (a) Canto, J. G.; Iskandrian, A. E. *J. Am. Med. Assoc.* **2003**, 290, 947; (b) Nabel, E. G. *N. Engl. J. Med.* **2003**, 349, 60.
- Davidson, M. H.; Robinson, J. G. *Expert Opin. Pharmacother.* **2006**, 7, 170.
- Tobert, J. A. *Nat. Rev. Drug Disc.* **2003**, 2, 517.
- Bays, H.; Stein, E. A. *Expert Opin. Pharmacother.* **2003**, 4, 1901.
- Eisele, B.; Budzinski, R.; Mueller, P.; Maier, R.; Mark, M. *J. Lipid Res.* **1997**, 38, 564.
- Mark, M.; Mueller, P.; Maier, R.; Eisele, B. *J. Lipid Res.* **1996**, 37, 148.
- Morand, O. H.; Aebi, J. D.; Dehmlow, H.; Ji, Y.-H.; Gains, N.; Lengsfeld, H.; Himber, J. *J. Lipid Res.* **1997**, 38, 373.
- Brown, G. R.; Hollinshead, D. M.; Stokes, E. S. E.; Clarke, D. S.; Eakin, M. A.; Foubister, A. J.; Glossop, S. C.; Griffiths, D.; Johnson, M. C.; McTaggart, F.; Mirrlees, D. J.; Smith, G. J.; Wood, R. *J. Med. Chem.* **1999**, 42, 1306.

9. Brown, G. R.; Hollinshead, D. M.; Stokes, E. S. E.; Waterson, D.; Clarke, D. S.; Foubister, A. J.; Glossop, S. C.; McTaggart, F.; Mirrlees, D. J.; Smith, G. J.; Wood, R. *J. Med. Chem.* **2000**, *43*, 4964.
10. Pyrah, I. T.; Kalinowski, A.; Jackson, D.; Davies, W.; Davis, S.; Aldridge, A.; Greaves, P. *Toxicol. Pathol.* **2001**, *29*, 174.
11. Phillips, W. A.; Avigan, J. *Proc. Soc. Exp. Biol. Med.* **1963**, *112*, 233.
12. Cenedella, R. J.; Bierkamper, G. G. *Exp. Eye Res.* **1979**, *28*, 673.
13. Cenedella, R. J.; Jacob, R.; Borchman, D.; Tang, D.; Neely, A. R.; Samadi, A.; Mason, R. P.; Sexton, P. *J. Lipid Res.* **2004**, *45*, 1232.
14. Cenedella, R. J. *Surv. Ophthalmol.* **1996**, *40*, 320.
15. Cenedella, R. J.; Kuszak, J. R.; Al-Ghoul, K. J.; Qin, S.; Sexton, P. S. *J. Lipid Res.* **2003**, *44*, 198.
16. Junk, J.; Landes, C. *Exp. Toxicol. Pathol.* **2005**, *57*, 29.
17. Gerson, R. J.; MacDonald, J. S.; Alberts, A. W.; Chen, J.; Yudkovitz, J. B.; Greenspan, M. D.; Rubin, L. F.; Bokelman, D. L. *Exp. Eye Res.* **1990**, *50*, 65.
18. Gerson, R. J.; Allen, H. L.; Lankas, G. R.; MacDonald, J. S.; Alberts, A. W.; Bokelman, D. L. *Fundam. Appl. Toxicol.* **1991**, *16*, 320.
19. (a) Dang, T.; Abe, I.; Zheng, Y. F.; Prestwich, G. D. *Chem. Biol.* **1999**, *6*, 333; (b) Lenhart, A.; Weihofen, W. A.; Pleschke, A. E. W.; Schulz, G. E. *Chem. Biol.* **2002**, *9*, 639–645.
20. Thoma, R.; Schulz-Gasch, T.; D'Arcy, B.; Benz, J.; Aebi, J.; Dehmlow, H.; Hennig, M.; Stihle, M.; Ruf, A. *Nature* **2004**, *432*, 118.
21. Mueller, R.; Huerzeler, M.; Boss, C. *Molecules* **2003**, *8*, 556.
22. Magdolen, P.; Meiarová, M.; Toma, T. *Tetrahedron* **2001**, *57*, 4781.
23. Pfoertner, K. H.; Bernauer, K.; Kaufmann, F.; Lorch, E. *Helv. Chim. Acta* **1985**, *68*, 584.